logs, including the second Z-DNA binding domain of ADAR1, Zβ, and the viral protein E3L (Fig. 4A).

The unique zigzag pattern of the sugar-phosphate backbone and the anti-syn alternation of the bases are characteristic of Z-DNA and distinguish it from other nucleic acid structures. The Zα domain has a tailored fit, which recognizes both features specifically. This binding can be generalized to other related left-handed Z-DNA binding HTH proteins and may provide a way to further explore the biological role(s) of Z-DNA.

References and Notes

1. A. H. Wang *et al.*, *Nature* **282**, 680 (1979).
2. A. G. Herbert, J. R. Spitzner, K. Lowenhaupt, A. Rich, *Proc. Natl. Acad. Sci. U.S.A.* **90**, 3339 (1993); A. Herbert, K. Lowenhaupt, J. Spitzner, A. Rich, *ibid.* **92**, 7550 (1995).
3. A. G. Herbert and A. Rich, *Nucleic Acids Res.* **21**, 2669 (1993).
4. A. Herbert *et al.*, *Proc. Natl. Acad. Sci. U.S.A.* **94**, 8421 (1997).
5. I. Berger *et al.*, *Biochemistry* **37**, 13313 (1998).
6. A. Herbert *et al.*, *Nucleic Acids Res.* **26**, 3486 (1998).
7. T. Schwartz *et al.*, *J. Biol. Chem.* **274**, 2899 (1999).
8. The protein construct used here was originally named Za (*7*). It is structurally homogeneous, unlike other published Zα peptides. For simplicity, here we use the generic name Zα instead of Za.
9. Guanine nucleotides are in the syn conformation characteristic of Z-DNA, with C3′-endo sugar puckers. In contrast to crystals containing Z-DNA without protein, the DNA in this crystal does not form continuous helices; instead it is stacked 3′ to 3′ with the stacked molecules slightly displaced laterally. In pure DNA crystals the phosphate group in G4pC5 is seen in two alternate conformations, Z_I and Z_{II} [A. J. Wang *et al.*, *Science* **211**, 171 (1981); R. V. Gessner, C. A. Frederick, G. J. Quigley, A. Rich, A. H. Wang, *J. Biol. Chem.* **264**, 7921 (1989)]. In the structure described here, this phosphate group is uniformly in the Z_I conformation as are all other phosphates at GpC steps. The Z_{II} conformation does not allow the interaction with Lys^{170}.
10. Two complexes (I, II) are related by a noncrystallographic twofold axis, and the third (III) resides on a crystallographic dyad. Some amino acids at the NH_2- and COOH-termini of the protein are disordered. The structure is defined for residues 134 to 198 of the Zα monomer in complex I, 136 to 199 in complex II, and 134 to 199 in complex III. The DNA structure is well resolved except for the 5′-dT overhang, which appears to be disordered.
11. M. Schade, C. J. Turner, K. Lowenhaupt, A. Rich, A. Herbert, *EMBO J.* **18**, 470 (1999).
12. S. K. Burley and G. A. Petsko, *Adv. Prot. Chem.* **39**, 125 (1988).
13. Single-letter abbreviations for amino acid residues are as follows: A, Ala; C, Cys; D, Asp; E, Glu; F, Phe; G, Gly; H, His; I, Ile; K, Lys; L, Leu; M, Met; N, Asn; P, Pro; Q, Gln; R, Arg; S, Ser; T, Thr; V, Val; W, Trp; and Y, Tyr.
14. Rmsd is 0.93 Å between complex I and II, 1.07 Å between complex II and III, and 0.76 Å between complex I and III, including all protein and DNA atoms, even though the three complexes were built and refined entirely independently.
15. When the Zα domain is superimposed on other proteins in the family, the similarity is most striking with the metallothionein transcriptional repressor SmtB (*17*) (rmsd 44 C^α atoms 0.79 Å), the catabolite gene activator protein CAP (*17*) (rmsd 43 C^α atoms 0.94 Å), and the related winged-helix class of proteins, such as hepatocyte nuclear factor HNF-3γ (*17*) (rmsd 30 C^α atoms 2.36 Å) and histone H5 (*17*) (rmsd 39 C^α atoms 1.28 Å).
16. D. M. J. Lilley, *DNA-Protein: Structural Interactions* (Oxford Univ. Press, Oxford, 1995).
17. Structures: HNF-3γ [K. L. Clark, E. D. Halay, E. Lai, S. K. Burley, *Nature* **364**, 412 (1993)], SmtB [W. J. Cook, S. R. Kar, K. B. Taylor, L. M. Hall, *J. Mol. Biol.* **275**, 337 (1998)], CAP [S. C. Schultz, G. C. Shields, T. A. Steitz, *Science* **253**, 1001 (1991)], H5 [V. Ramakrishnan, J. T. Finch, V. Graziano, P. L. Lee, R. M. Sweet, *Nature* **362**, 219 (1993)], OCT-1 [J. D. Klemm, M. A. Rould, R. Aurora, W. Herr, C. O. Pabo, *Cell* **77**, 21 (1994)], and PAX-6 [H. E. Xu *et al.*, *Genes Dev.*, in press].
18. S. C. Harrison and A. K. Aggarwal, *Annu. Rev. Biochem.* **59**, 933 (1990); C. O. Pabo and R. T. Sauer, *ibid.* **61**, 1053 (1992).
19. D. E. Draper and L. P. Reynaldo, *Nucleic Acids Res.* **27**, 381 (1999); S. K. Chan and G. Struhl, *Nature* **388**, 634 (1997); D. A. Wah, J. A. Hirsch, L. F. Dorner, I. Schildkraut, A. K. Aggarwal, *ibid.*, p. 97.
20. Program tools: X-PLOR [A. T. Brünger, *X-PLOR Version 3.1. A System for X-ray Crystallography and NMR* (Yale Univ. Press, New Haven, CT, 1992)], HKL package [Z. Otwinowski and W. Minor, *Methods Enzymol.* **276A**, 307 (1997)], SOLVE [T. C. Terwilliger and J. Berendzen, *Acta Crystallogr.* **D52**, 749 (1996)], DM [K. Cowtan and P. Main, *ibid.*, p. 43 (1996)], and Procheck [A. L. Morris, M. W. MacArthur, E. G. Hutchinson, J. M. Thornton, *Proteins* **12**, 345 (1992)].
21. For example, in the engrailed homeodomain-DNA complex, 960 $Å^2$ of protein surface area is lost upon binding [E. Fraenkel, M. A. Rould, K. A. Chambers, C. O. Pabo, *J. Mol. Biol.* **284**, 351 (1998)].
22. The dissociation constant for Zα bound to a 6-bp DNA duplex $d(CGCGCG)_2$ is 30 nM, as determined by ultracentrifugation (M. Schade *et al.*, unpublished data).
23. L. F. Liu and J. C. Wang, *Proc. Natl. Acad. Sci. U.S.A.* **84**, 7024 (1987); B. Wittig, T. Dorbic, A. Rich, *ibid.* **88**, 2259 (1991); B. Wittig, S. Wölfl, T. Dorbic, W. Vahrson, A. Rich, *EMBO J.* **11**, 4653 (1992).
24. S. Maas, T. Melcher, P. H. Seeburg, *Curr. Opin. Cell Biol.* **9**, 343 (1997).
25. A. Herbert and A. Rich, *J. Biol. Chem.* **271**, 11595 (1996).
26. T. Schwartz *et al.*, *Acta Crystallogr.*, in press.
27. Figures were made with MOLSCRIPT (Figs. 1 and 2A) [P. J. Kraulis, *J. Appl. Crstallogr.* **24**, 946 (1991)], Bobscript (Fig. 3A) [R. M. Esnouf, *J. Mol. Graphics* **15**, 132 (1997)], and RASTER-3D [E. A. Merritt and E. P. Murphy, *Acta Crystallogr. D* **50**, 869 (1994)]. Figure 3B was made with GRASP [A. Nicholls, K. A. Sharp, B. Honig, *Proteins Struct. Funct. Genet.* **11**, 281 (1991)].

28. Supported by grants from the National Institutes of Health and the National Science Foundation and by a fellowship from the German Academic Exchange Service (DAAD) to T.S. Coordinates for the crystal structure have been deposited in the Protein Data Bank (accession code 1QBJ).

5 March 1999; accepted 29 April 1999

Specific Coupling of NMDA Receptor Activation to Nitric Oxide Neurotoxicity by PSD-95 Protein

Rita Sattler,[1] Zhigang Xiong,[2] Wei-Yang Lu,[2] Mathias Hafner,[3] John F. MacDonald,[2] Michael Tymianski[1]*

The efficiency with which *N*-methyl-D-aspartate receptors (NMDARs) trigger intracellular signaling pathways governs neuronal plasticity, development, senescence, and disease. In cultured cortical neurons, suppressing the expression of the NMDAR scaffolding protein PSD-95 (postsynaptic density–95) selectively attenuated excitotoxicity triggered via NMDARs, but not by other glutamate or calcium ion (Ca^{2+}) channels. NMDAR function was unaffected, because receptor expression, NMDA currents, and $^{45}Ca^{2+}$ loading were unchanged. Suppressing PSD-95 blocked Ca^{2+}-activated nitric oxide production by NMDARs selectively, without affecting neuronal nitric oxide synthase expression or function. Thus, PSD-95 is required for efficient coupling of NMDAR activity to nitric oxide toxicity, and imparts specificity to excitotoxic Ca^{2+} signaling.

Calcium influx through NMDARs plays key roles in synaptic transmission, neuronal development, and plasticity (*1*). Excessive Ca influx triggers excitotoxicity (*2*), damaging neurons in diverse neurological disorders (*3*). Rapid Ca^{2+}-dependent neurotoxicity is triggered most efficiently when Ca^{2+} influx occurs through NMDARs, and cannot be reproduced by loading neurons with equivalent quantities of Ca^{2+} through non-NMDARs or voltage-sensitive Ca^{2+} channels (VSCCs) (*4*). This suggests that Ca^{2+} influx through NMDAR channels is functionally coupled to neurotoxic signaling pathways.

We hypothesized that lethal Ca^{2+} signaling by NMDARs is determined by the molecules with which they interact. The NR2 NMDAR subunits bind to PSD-95/SAP90 (*5*), chapsyn-110/PSD-93, and other members of the membrane-associated guanylate

[1]Toronto Western Hospital, University of Toronto, Lab 11-416, 399 Bathurst Street, Toronto, Ontario M5T 2S8, Canada. [2]Department of Physiology, University of Toronto, Toronto, Ontario M5G 1X8, Canada. [3]Mannheim University of Applied Sciences, 68163 Mannheim, Germany.

*To whom correspondence should be addressed. E-mail: mike_t@playfair.utoronto.ca

kinase (MAGUK) family (*6*). NMDAR-bound MAGUKs are generally distinct from those associated with non-NMDARs (*7*). This raises the possibility that the preferential activation of neurotoxic Ca^{2+} signals by NMDARs is determined by the distinctiveness of NMDAR-bound MAGUKs, or of the intracellular proteins that they bind. We thus focused on PSD-95, an abundant scaffolding molecule that binds and clusters NMDARs preferentially and may link them to intracellular signaling molecules (*8*).

With the use of a 15-nucleotide oligomer phosphodiester antisense oligodeoxynucleotide (ODN), PSD-95 expression was suppressed in cultured cortical neurons to <10% of expression in controls (Fig. 1, A and B) (*9*, *10*). Sham washes had no effect, nor did sense and missense ODNs (*9*). The ODNs had no effect on neuronal survivability and morphology, as gauged by viability assays (below) and phase-contrast microscopy (*11*).

To examine the impact of PSD-95 on NMDAR-triggered excitotoxicity, we exposed ODN-treated cultures to NMDA (10 to 100 μM) for 60 min; after washing, these cultures were either used for $^{45}Ca^{2+}$ accumulation measurements or observed for a further 23 hours (*12*). Ca^{2+} influx was isolated to NMDARs by adding antagonists of non-NMDARs and Ca^{2+} channels (*4*, *12*). NMDA toxicity was significantly reduced in neurons deficient in PSD-95 across a range of insult severities (Fig. 1, C and D) [median effective concentration (EC_{50}): antisense, 43.2 ± 4.3 μM; sense, 26.3 ± 3.4 μM; Bonferroni *t* test, $P < 0.005$] (*13*). However, PSD-95 deficiency had no effect on Ca^{2+} loading into identically treated sister cultures (Fig. 1E). Therefore, PSD-95 deficiency induces resilience to NMDA toxicity despite maintained Ca^{2+} loading.

We next examined whether the increased resilience to Ca^{2+} loading in PSD-95–deficient neurons was specific to NMDARs. Non-NMDAR toxicity was produced using kainic acid (30 to 300 μM) (*14*) in the presence of NMDAR and Ca^{2+} channel antagonists (*4*, *12*). Kainate toxicity was unaffected in PSD-95–deficient neurons challenged for either 60 min (*11*) or 24 hours (Fig. 2A). Non-NMDAR toxicity occurred without significant $^{45}Ca^{2+}$ loading (Fig. 2B), as >92% of neurons in these cultures express Ca^{2+}-impermeable AMPA receptors (*4*). However, Ca^{2+} loading through VSCCs, which is nontoxic (*4*) (Fig. 2C), was also unaffected by PSD-95 deficiency (Fig. 2D). Thus, suppressing PSD-95 expression affects neither the toxicity nor Ca^{2+} fluxes triggered through pathways other than NMDARs.

Immunoblot analysis (*10*) of PSD-95–deficient cultures revealed no alterations in the expression of the essential NMDAR subunit NR1, nor of two other NMDAR-associated MAGUKs, PSD-93 and SAP-102 (Fig. 3A). This indicated that altered expression of NMDARs and their associated proteins was unlikely to explain the reduced toxicity of NMDA in PSD-95 deficiency. Therefore, we examined whether PSD-95 modulates NMDAR function (*15*). NMDA currents were

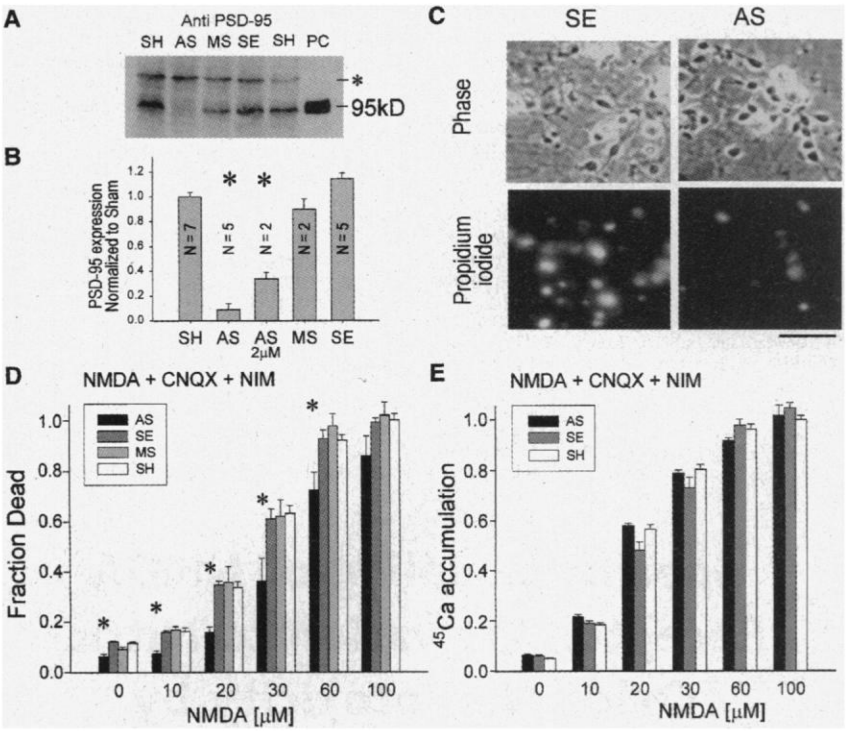

Fig. 1. Increased resilience of PSD-95–deficient neurons to NMDA toxicity despite Ca^{2+} loading. (**A**) Immunoblot showing representative effects of PSD-95 antisense (AS), sense (SE), and missense (MS) ODNs, as well as sham (SH) washes, on PSD-95 expression. PC, positive control tissue from purified rat brain cell membranes. Asterisk: nonspecific band produced by the secondary antibody, useful to control for protein loading and blot exposure times. (**B**) Densitometric analysis of PSD-95 expression pooled from *N* experiments. Asterisk: different from other groups, ANOVA, $F = 102$, $P < 0.0001$. ODNs were used at 5 μM except where indicated (AS, 2 μM). (**C**) Representative phase contrast and propidium iodide fluorescence images of PSD-95–deficient (AS) and control (SE) cultures 24 hours after a 60-min challenge with 30 μM NMDA. Scale bar, 100 μm. (**D**) Decreased NMDA toxicity at 24 hours in PSD-95–deficient neurons [with CNQX and nimodipine (NIM) added as described (*12*)] after selective NMDAR activation for 60 min (16 cultures per bar, pooled from four independent experiments). Asterisk: differences from SE, MS, and SH (Bonferroni *t* test, $P < 0.005$). (**E**) No effect of suppressing PSD-95 on NMDAR-mediated Ca^{2+} loading (12 cultures per bar from three independent experiments).

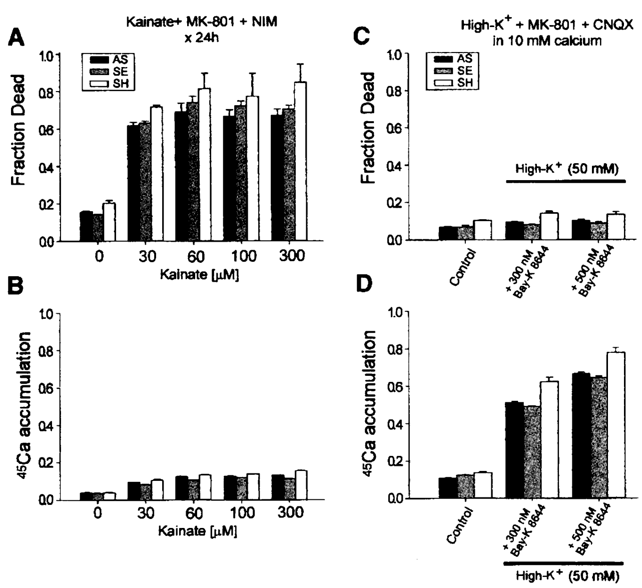

Fig. 2. PSD-95 deficiency does not affect toxicity and Ca^{2+} loading produced by activating non-NMDARs and Ca^{2+} channels. Cultures were treated with sham washes or antisense or sense ODNs as in Fig. 1. (**A** and **B**) Selective activation of AMPA/kainate receptors with kainate plus MK-801 and nimodipine produces toxicity over 24 hours (A) irrespective of PSD-95 deficiency, with minimal $^{45}Ca^{2+}$ loading (B). (**C** and **D**) Selective activation of VSCCs (*12*) produces little toxicity (C), but significant $^{45}Ca^{2+}$ loading (D) that is also insensitive to PSD-95 deficiency. Four cultures are represented per bar in all experiments.

recorded using the whole-cell patch technique (*16*) (Fig. 3B). PSD-95 deficiency had no effect on passive membrane properties, including input resistance and membrane capacitance {capacitance: antisense, 55.0 ± 2.6 pF; sense, 52.7 ± 3.2 pF; sham, 48.1 ± 3.4 pF [17 to 19 neurons per group; analysis of variance (ANOVA), $F = 1.29$, $P = 0.28$]}. Whole-cell currents elicited with 3 to 300 μM NMDA were also unaffected. Peak currents were as follows: antisense, 2340 ± 255 pA; sense, 2630 ± 276 pA; sham, 2370 ± 223 pA (Fig. 3B, right; 17 to 19 neurons per group; ANOVA, $F = 0.43$, $P = 0.65$). NMDA dose-response relationships also were unchanged [Fig. 3B, left; EC_{50} antisense, 16.1 ± 0.8 μM, sense, 15.5 ± 2.1 μM; sham, 15.9 ± 2.9 μM (six to nine neurons per group; one-way ANOVA, $F = 0.02$, $P = 0.98$)], as were NMDA current density and desensitization (Fig. 3C).

To further examine the effect of PSD-95 binding on NMDAR function, we injected a nine–amino acid peptide (Lys-Leu-Ser-Ser-Ile-Glu-Ser-Asp-Val) corresponding to the COOH-terminal domain of the NR2B subunit characterized by the tSXV motif (*6*) into the neurons. At 0.5 mM, this peptide competitively inhibited the binding of PSD-95 to GST-NR2B fusion proteins (*6*) and was therefore predicted to uncouple NMDARs from PSD-95. Intracellular dialysis of 1 mM tSXV or control peptide (Cys-Ser-Lys-Asp-Thr-Met-Glu-Lys-Ser-Glu-Ser-Leu) (*6*) was achieved through patch pipettes (3 to 5 megohms) also containing the fluorescent tracer Lucifer Yellow. This had no effect on NMDA currents over 30 min, despite extensive dialysis of Lucifer Yellow into the cell soma and dendrites (Fig. 3D). Peak current amplitudes were as follows: tSXV, 2660 ± 257 pA ($n = 9$); control, 2540 ± 281 pA ($n = 10$; $t_{(17)} = 0.31$, $P = 0.76$).

Consistent with data obtained from recently generated mutant mice expressing a truncated 40K PSD-95 protein (*17*), we found no effects of PSD-95 deficiency on NMDAR expression, on other NMDAR-associated MAGUKs, or on NMDA-evoked currents. In addition, NMDAR function gauged by measuring NMDA-evoked $^{45}Ca^{2+}$ accumulation was unaffected. Thus, the

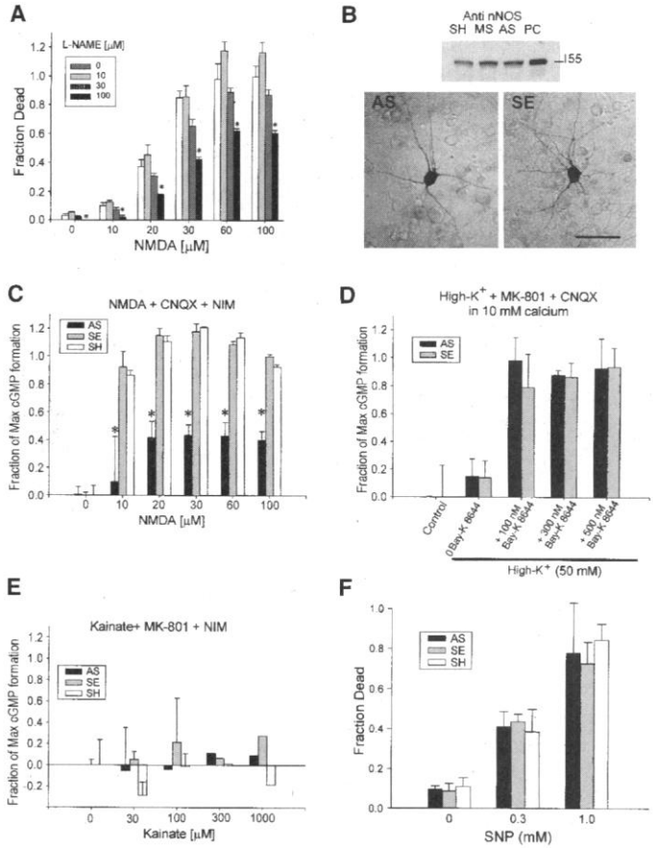

Fig. 4. Coupling of NMDAR activation to nitric oxide signaling by PSD-95. **(A)** L-NAME protects against NMDA toxicity (eight cultures per bar). Asterisk: difference from 0 μM L-NAME (Bonferroni *t* test, $P < 0.05$). **(B)** No effect of sham washes and of PSD-95 antisense and missense ODNs on nNOS expression (immunoblot) and of antisense and sense ODNs on NADPH diaphorase staining. **(C)** Effect of selective NMDAR activation (*12*) on cGMP formation (12 cultures per bar). **(D and E)** Effects of VSCC activation (eight cultures per bar) and selective AMPA/kainate receptor activation (*12*) (four cultures per bar, one experiment) on cGMP formation. Data in (C) to (E) are expressed as the fraction of cGMP produced in sense-treated cultures by 100 μM NMDA. Asterisk: differences from both sham and sense controls (Bonferroni *t* test, $P < 0.0001$). **(F)** Sodium nitroprusside toxicity is similar in PSD-95 antisense-, sense-, and sham-treated cultures. Data in all bars in (A), (C), (D), and (F) were pooled from two or three independent experiments.

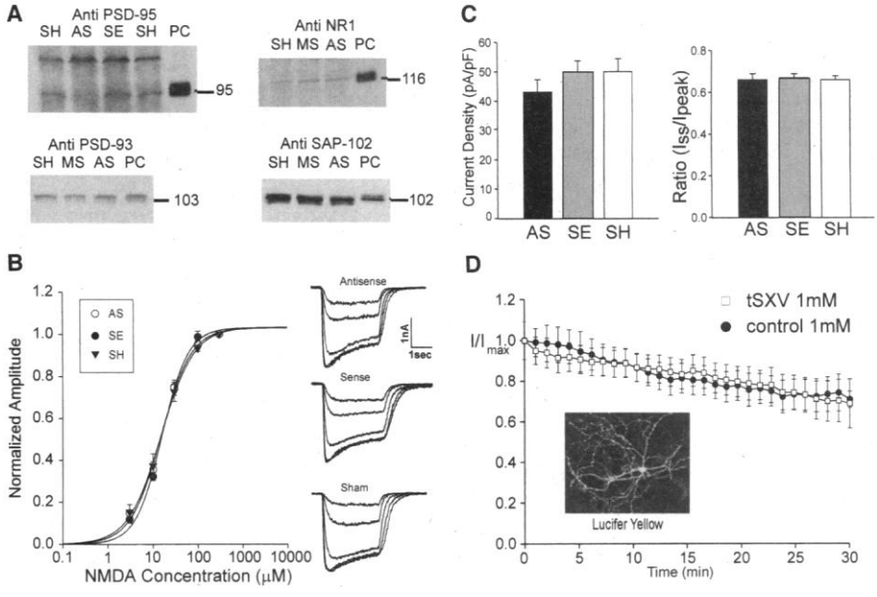

Fig. 3. Perturbing PSD-95 has no effect on NMDA receptor function. **(A)** Immunoblots of PSD-95 ODN-treated cultures probed for PSD-95, NR1, PSD-93, and SAP-102. PC, positive control from purified rat brain cell membranes; other abbreviations as in Figs. 1 and 2. **(B)** NMDA dose-response curves (left) and representative NMDA currents (right) obtained with 3 to 300 μM NMDA. **(C)** Measurements of NMDA (300 μM) current density (17 to 19 neurons per group; ANOVA, $F = 1.10$, $P = 0.34$) and of NMDA current desensitization. I_{ss}, steady-state current; I_{peak}, peak current (15 to 16 neurons per group; ANOVA, $F = 0.14$, $P = 0.87$). Time constants for current decay: antisense, 1310 ± 158 ms; sense, 1530 ± 185 ms; sham, 1190 ± 124 ms (ANOVA, $F = 1.22$, $P = 0.31$). **(D)** Currents elicited with 300 μM NMDA in neurons dialyzed with Lucifer Yellow (inset) and 1 mM tSXV or control peptide.

neuroprotective consequences of PSD-95 deficiency must be due to events downstream from NMDAR activation.

The second PDZ domain of PSD-95 binds to the COOH-terminus of NR2 subunits and to other intracellular proteins (*8*). Among these is neuronal nitric oxide synthase (nNOS) (*18*), an enzyme that catalyzes nitric oxide (NO) production (*19*). Although never demonstrated experimentally, the NMDAR–PSD-95–nNOS complex was postulated to account for the preferential production of NO by NMDARs over other pathways (*8*). To determine whether NO signaling plays a role in NMDA toxicity in the present cultures, we treated the cells with *N*-nitro-L-arginine methyl ester (L-NAME), a NOS inhibitor (*19*). Because L-NAME protected the neurons against NMDA toxicity (Fig. 4A), it is possible that suppression of PSD-95 might perturb this toxic signaling pathway.

The effect of suppressing PSD-95 expression on NO signaling and toxicity was examined using guanosine 3′,5′-monophosphate (cGMP) formation as a surrogate measure of NO production by Ca^{2+}-activated nNOS (*20, 21*). PSD-95 deficiency had no impact on nNOS expression (Fig. 4B), nor on the morphology (Fig. 4B) or counts of the reduced form of nicotinamide adenine dinucleotide phosphate (NADPH) diaphorase–staining (*19*) neurons (sham, 361 ± 60; sense, 354 ± 54; antisense, 332 ± 42 staining neurons per 10-mm cover slip, three cover slips per group). However, in neurons lacking PSD-95 challenged with NMDA under conditions that isolated Ca^{2+} influx to NMDARs (*4*), cGMP production was markedly attenuated (>60%; ANOVA, $P < 0.0001$) (Fig. 4C). Like inhibited toxicity, inhibited cGMP formation in neurons lacking PSD-95 was only observed in response to NMDA. It was unaffected in neurons loaded with Ca^{2+} through VSCCs (Fig. 4D), even under high neuronal Ca^{2+} loads matching those attained by activating NMDARs (compare Figs. 1E and 2D) (*4*). Therefore, nNOS function was unaffected by PSD-95 deficiency. AMPA/kainate receptor activation failed to load the cells with Ca^{2+} (Fig. 2B) and thus failed to increase cGMP concentrations (Fig. 4E). Suppressing PSD-95 thus selectively reduces NO production efficiency by NMDAR-mediated Ca^{2+} influx, but preserves NO production by Ca^{2+} influx through other pathways.

Bypassing nNOS activation with NO donors restored toxicity in neurons lacking PSD-95. The NO donors sodium nitroprusside (*19*) (Fig. 4F; EC_{50} = 300 μM) and *S*-nitrosocysteine (*11, 22*) were highly toxic, irrespective of PSD-95 deficiency. Thus, reduced NMDA toxicity in PSD-95–deficient cells was unlikely to be caused by altered signaling events downstream from NO formation.

Suppressing PSD-95 expression uncoupled NO formation from NMDAR activation (Fig. 4C), and also protected neurons against NMDAR toxicity (Fig. 1, C and D) without affecting receptor function (Fig. 1E and Fig. 3, A to D), by mechanisms downstream from NMDAR activation and upstream from NO-mediated toxic events (Fig. 4F). Therefore, PSD-95 imparts signaling and neurotoxic specificity to NMDARs through the coupling of receptor activity to critical second messenger pathways. Our results have broader consequences, in that NMDAR activation and NO signaling are also critical to neuronal plasticity, learning, memory, and behavior (*1, 20, 23*). Thus, our report provides evidence for a potential mechanism by which PSD-95 may govern important physiological and pathological aspects of neuronal functioning.

References and Notes

1. A. Ghosh and M. E. Greenberg, *Science* **268**, 239 (1995); T. V. Bliss and G. L. Collingridge, *Nature* **361**, 31 (1993).
2. J. W. Olney, *Kainic Acid as a Tool in Neurobiology*, E. G. McGeer, J. W. Olney, P. L. McGeer, Eds. (Raven, New York, 1978), pp. 95–121; S. M. Rothman and J. W. Olney, *Trends Neurosci.* **10**, 299 (1987); D. W. Choi, *Ann. N.Y. Acad. Sci.* **747**, 162 (1994).
3. S. A. Lipton and P. A. Rosenberg, *N. Engl. J. Med.* **330**, 613 (1994).
4. R. Sattler, M. P. Charlton, M. Hafner, M. Tymianski, *J. Neurochem.* **71**, 2349 (1998); M. Tymianski, M. P. Charlton, P. L. Carlen, C. H. Tator, *J. Neurosci.* **13**, 2085 (1993).
5. K. O. Cho, C. A. Hunt, M. B. Kennedy, *Neuron* **9**, 929 (1992).
6. H. C. Kornau, L. T. Schenker, M. B. Kennedy, P. H. Seeburg, *Science* **269**, 1737 (1995); J. E. Brenman, K. S. Christopherson, S. E. Craven, A. W. McGee, D. S. Bredt, *J. Neurosci.* **16**, 7407 (1996); B. M. Muller *et al.*, *Neuron* **17**, 255 (1996).
7. H. Dong *et al.*, *Nature* **386**, 279 (1997); P. R. Brakeman *et al.*, *ibid.*, p. 284.
8. S. E. Craven and D. S. Bredt, *Cell* **93**, 495 (1998); M. Niethammer *et al.*, *Neuron* **20**, 693 (1998); J. H. Kim, D. Liao, L. F. Lau, R. L. Huganir, *ibid.*, p. 683; T. Tezuka, H. Umemori, T. Akiyama, S. Nakanishi, T. Yamamoto, *Proc. Natl. Acad. Sci. U.S.A.* **96**, 435 (1999).
9. Cultured cortical neurons were prepared by standard techniques (*4*) and switched to serum-free media at 24 hours (Neurobasal with B27 supplement, Gibco). The antisense ODN corresponded to nucleotides 435 to 449 (5′-GAATGGGTCACCTCC-3′) of mouse PSD-95/SAP90 mRNA (GenBank accession number D50621). Filter-sterilized phosphodiester antisense, sense, and missense (5′-CCGCTCTATCGAGGA-3′) ODNs (5 μM) were added in culture medium during feedings at 4, 6, 8, and 10 days after plating. Cultures were used for all experiments (Figs. 1 to 4) on day 12. ODN sequences exhibited no similarity to any other known mammalian genes {BLAST search [S. F. Altschul *et al.*, *Nucleic Acids Res.* **25**, 3389 (1997)]}.
10. Immunoblotting was performed as described [O. T. Jones *et al.*, *J. Neurosci.* **17**, 6152 (1997)]. Tissue was harvested and pooled from two cultures per lane. The blotted proteins were probed using a monoclonal antibody (mAb) to PSD-95 (1:250 dilution) [mouse immunoglobulin G1 (IgG1), Transduction Labs], polyclonal antibodies to PSD-93 (1:1000 dilution) and SAP-102 (1:2000 dilution) (rabbit serum, Synaptic Systems GmbH), an NR1 mAb (1:1000 dilution) (mouse IgG2a, Pharmingen Canada), or an nNOS (NOS type I) mAb (1:2500 dilution) (mouse IgG2a, Transduction Labs). Secondary antibodies were sheep antibody to mouse Ig or donkey antibody to rabbit Ig, conjugated to horseradish peroxidase (Amersham). Immunoblots for PSD-95 were obtained for all experiments (Figs. 1 to 4) from sister cultures, and all gels were quantified using an imaging densitometer (Bio-Rad GS-670).
11. M. Tymianski and R. Sattler, unpublished data.
12. Excitotoxicity and Ca^{2+} accumulation measurements were performed as described (*4*) [R. Sattler, M. P. Charlton, M. Hafner, M. Tymianski, *J. Cereb. Blood Flow Metab.* **17**, 455 (1997)] using measurements of propidium iodide fluorescence and of radiolabeled $^{45}Ca^{2+}$ accumulation, respectively. Each was expressed as the fraction of maximum propidium iodide fluorescence and $^{45}Ca^{2+}$ accumulation achievable in sister cultures exposed to 100 μM NMDA for 60 min, which kills >95% of neurons. Experimental solutions were as described (*4*). Ca^{2+} influx was isolated to distinct pathways as follows: To NMDARs by applying NMDA (for 60 min) with 6-cyano-7-nitroquinoxaline-2,3-dione (CNQX, an AMPA/kainate antagonist; RBI) and nimodipine (a Ca^{2+} channel antagonist; Miles Pharmaceuticals), to non-NMDARs by applying kainic acid (for 60 min or 24 hours) with MK-801 (an NMDA antagonist; RBI) and nimodipine, and to VSCCs using 50 mM K^+ solution (for 60 min) containing 10 mM Ca^{2+} and S(-)-Bay K 8644, an L-type channel agonist (300 to 500 nM; RBI), MK-801, and CNQX. Antagonist concentrations were 10 μM MK-801, 10 μM CNQX, and 2 μM nimodipine. All three antagonists were added after the 60-min agonist applications for the remainder of all experiments (24 hours). All drug concentrations and the insult duration were chosen to conform with previous experiments that established the finding of preferential activation of Ca^{2+}-mediated toxicity by NMDAR activation (*4*).
13. All data were analyzed by ANOVA, with a post hoc Student's *t* test using the Bonferroni correction for multiple comparisons. Means are presented with their standard errors.
14. N. Burnashev, Z. Zhou, E. Neher, B. Sakmann, *J. Physiol.* **485**, 403 (1995).
15. Y. Yamada, Y. Chochi, K. Takamiya, K. Sobue, M. Inui, *J. Biol. Chem.* **274**, 6647 (1999).
16. Whole-cell patch-clamp recordings were performed and analyzed as described [Z. Xiong, W. Lu, J. F. MacDonald, *Proc. Natl. Acad. Sci. U.S.A.* **94**, 7012 (1997)]. During each experiment, a voltage step of −10 mV was applied from holding potential and the capacitative transient was integrated to obtain cell capacitance. The extracellular solution contained 140 mM NaCl, 5.4 mM KCl, 1.3 mM $CaCl_2$, 25 mM Hepes, 33 mM glucose, 0.01 mM glycine, and 0.001 mM tetrodotoxin (pH = 7.3 to 7.4, 320 to 335 mosM). Solutions containing NMDA were rapidly exchanged with a multibarrel perfusion system. The pipette solution contained 140 mM CsF, 35 mM CsOH, 10 mM Hepes, 11 mM EGTA, 2 mM tetraethylammonium chloride (TEA), 1 mM $CaCl_2$, and 4 mM Mg–adenosine triphosphate (pH 7.3, 300 mosM). Lucifer Yellow (0.5% w/v) was included in the pipette for experiments in Fig. 3D.
17. M. Migaud *et al.*, *Nature* **396**, 433 (1998).
18. J. E. Brenman *et al.*, *Cell* **84**, 757 (1996).
19. V. L. Dawson, T. M. Dawson, E. D. London, D. S. Bredt, S. H. Snyder, *Proc. Natl. Acad. Sci. U.S.A.* **88**, 6368 (1991); V. L. Dawson, T. M. Dawson, D. A. Bartley, G. R. Uhl, S. H. Snyder, *J. Neurosci.* **13**, 2651 (1993); T. M. Dawson, D. S. Bredt, M. Fotuhi, P. M. Hwang, S. H. Snyder, *Proc. Natl. Acad. Sci. U.S.A.* **88**, 7797 (1991).
20. S. R. Jaffrey and S. H. Snyder, *Annu. Rev. Cell Dev. Biol.* **11**, 417 (1995).
21. cGMP determinations were performed 10 min after challenging the cultures with NMDA, kainate, or high-K (Fig. 4, C to E) with the Biotrak cGMP enzyme-immunoassay system using the manufacturer's instructions (Amersham). Staining for NADPH diaphorase (Fig. 4B) was done as described (*19*).
22. J. R. Brorson, P. T. Schumacker, H. Zhang, *J. Neurosci.* **19**, 147 (1999).
23. R. J. Nelson *et al.*, *Nature* **378**, 383 (1995).

24. Supported by NIH grant NS 39060 (M.T.) and MRC (J.F.M.). We thank O. T. Jones and K. Iihara for technical assistance, and D. W. Choi, M. W. Salter, and Y. T. Wang for critical comments on the manuscript. R.S. is a student, and W.Y.L. a fellow, of the Ontario Heart and Stroke Foundation. Z.X. is an MRC Centennial Fellow. M.T. is an MRC Clinician-Scientist.

22 March 1999; accepted 4 May 1999